Contents lists available at GrowingScience

Engineering Solid Mechanics

homepage: www.GrowingScience.com/esm

Shaft fatigue life and efficiency improvement of a micro cross flow turbine

A. Reihani, A. Ojaghi, S. Derakhshan and B. Beigzadeh*

School of Mechanical Engineering, Iran University of Science and Technology, Tehran, Iran

ARTICLE INFO

Article history:
Received September 20, 2013
Received in Revised form
October, 14, 2013
Accepted 20 December 2013
Available online
1 January 2014

Keywords:
Shaft Fatigue Life
Cross Flow Turbine
Multidisciplinary Optimization
Artificial Neural Network

ABSTRACT

The present study deals with optimization of hydraulic efficiency and shaft fatigue life of a micro cross-flow hydraulic turbine. A micro cross-flow turbine (KTP-B60) with shaft fatigue failure was considered as a case study. Numerical flow simulations were performed using a 3D-two phase flow solver, and the results have shown a good agreement with experimental data. Using an analytical method, the shaft fatigue factor of safety (FOS) was extracted from numerical simulation. CFD results were utilized in the optimization process in order to improve hydraulic efficiency and shaft fatigue life simultaneously using a meta- model (Artificial Neural Network) and genetic algorithm (GA). The priority of hydraulic efficiency and shaft fatigue life was altered by defining different objective functions in the optimization process. In one of the cases comparison of initial and optimal turbine showed a hydraulic efficiency improvement of 10.14 % and relative shaft FOS improvement of 4.86 %. The proposed optimization method could be exploited as an efficient and low cost procedure for energy generation improvement in micro hydro turbines.

1. Introduction

Application of micro hydro turbines as a renewable energy source has drawn worldwide attention during the last decades. Hydropower is one of the oldest energy resources known to the human, which offers a clean, non-polluting and almost endless source of energy. Energy production by burning of fossil fuels is the leading cause of climate change, and using hydropower is regarded as a viable solution to this ever increasing problem. Currently hydro-electric power is far and away the main renewable energy resource in use, satisfying two-thirds of all renewable electricity production in United States. Besides being emission-free, hydropower provides numerous benefits such as simple design and relatively simple manufacturing processes, low price per kW, easy installation without requiring heavy construction activities, cheap and easy maintenance, minimal or rather non-riverine impacts, being entirely domestic and decentralized, excellent reliability and proper energy

* Corresponding author.
E-mail addresses: b_beigzadeh@iust.ac.ir (B. Beigzadeh)

doi: 10.5267/j.esm.2014.1.001

efficiency properties have made them attractive especially to the countries with ample micro hydro sites (Lal 1975; Kosnik 2008; Yassi 2009; Yassi 2010).

There have been many researches about micro hydraulic turbines as the main equipment of a micro hydroelectric power plant, to utilize effectively as micro and off-grid power systems, e. g. Savonius turbine (Nakajima et al., 2008 a,b), pump reversed turbine (Derakhshan and Nourbakhsh, 2008), counter-rotating turbine (Kanemoto et al., 2007), Darrieus turbine (Takamatsu et al., 1991; Furukawa & Okuma, 1995; Matsuura et al., 2006), Gyro-type turbine (Kanemoto et al., 2004; Inagaki and Kanemoto, 2005), positive displacement turbine (Phommachamh et al., 2006) and Banki turbine (Pasandideh Pour, 2012). An extensive bibliographical review on the development of the cross-flow turbines can be found in the works of Khosrowpanah et al (1988), Fiuzat and Akerkar (1989,1991), and Desai and Aziz (1994). The works included details concerning the influence of the number of blades, outside diameter of the runner and admission arc of the nozzle on the turbine efficiency.

Nowadays the improvement of numerical simulation tools has allowed high accuracy in prediction of flow field in turbomachinery than previously attained. Using CFD methods, designers are able to predict hydraulic performance of turbines. However due to the complicated nature of free surface flow, numerical methods have slowly emerged in this regard. Utilization of CFD tools provides the opportunity to investigate the effect of each turbine component on overall hydraulic performance. Based on previously performed researches such as Costa Pereira and Borges (1996) and Choi et al., (2008), it has been found that nozzle shape could have a profound impact on the flow condition and hydraulic performance. On the other hand many researchers have utilized shape optimization as an effective approach in order to maximize the performance of turbomachinery such as researches performed by Derakhshan et al. (2008), Nourbakhsh et al. (2011) and Demeulenaere et al. (2004) in order to improve pump hydraulic efficiency.

In this paper, a KTP-B60 micro cross flow turbine with shaft failure issue has been taken as a case study. An optimization process was utilized to improve both hydraulic efficiency and shaft fatigue life using a meta- model (Artificial Neural Network) and genetic algorithm (GA) in conjunction with a verified numerical two phase flow solver. In order to determine the characteristics of the optimal turbine, performance curves have been extracted from CFD simulations. Results have shown that the suggested method is an efficient and reliable approach for optimization of micro hydraulic turbines.

2. Cross-flow turbine

Cross-flow turbine, known as Michell-Banki or Ossberger turbine, was first proposed in 1918 (Banki, 1918) which is categorized as an impulse turbine that operates in atmospheric pressure. Shepherd (1956) comments that in cross-flow turbines 75% of the available energy is transferred with higher efficiency in the first stage, when the water flows towards the interior of the runner, the remaining 25% is transferred with lower efficiency in the second stage. A schematic of the flow direction inside the turbine runner is depicted in Fig.1.

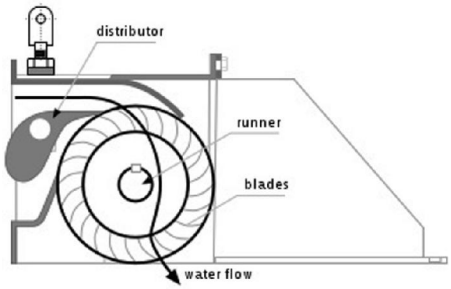

Fig. 1. Flow direction inside a cross-flow turbine runner (Penche, 1994)

3. Case study

The case study involves a KTP-B60 micro cross-flow turbine, which was formerly installed and exploited. The runner diameter is d = 300 mm and its length is L = 177.6 mm with total number of 19 blades and angles of $\beta_1 = 30° \; and \; \beta_2 = 90°$. The nozzle consists of a standard hydrofoil with $\theta_1 = 16°$ stagger angle and passage angles of $\theta_2 = 24°$ and $\theta_3 = 11°$. Overall turbine geometry is illustrated in Fig. 2. The rotational speed, flow rate, head, specific speed and shaft power of this turbine are 1000 rpm, 200 lit/s, 60 m, 45 and 61 kW respectively. Characteristic curves of this turbine are available in the section 3.2.3 which indicates a maximum efficiency of 51.6 % that may be unsatisfactory.

Fig. 2. KTP-B60 turbine (Pasandideh Pour, 2012)

During operation period several shaft failure reports were received which resulted in redesigning and substitution of this component for many times. However none of them were sufficiently durable. Insufficiency of mechanical design efforts resulted in a conclusion that the flow condition inside the runner is the major cause of this issue. On the other hand failure pattern and location indicates that this problem is caused due to fatigue which may be a result of fluctuating hydrodynamic forces caused by water jet impact to the shaft. Based on former studies which have demonstrated the profound impact of nozzle shape on flow path inside the runner, a decision was made to alter the nozzle shape in order to improve both shaft fatigue life and hydraulic efficiency of the turbine.

4. Optimization process

Fig. 3 shows the developed numerical optimization package including the parameterization, CFD, ANN and GA modules for the shape optimization of an initial turbine geometry. The details of the developed package are described in the following sections.

4.1 Geometry parameterization

In the optimization process the following geometry parameters were altered within a specific scope which is indicated in Table 1. Scopes of each parameter are selected to the extent that the boundaries would not intersect. As indicated in Fig. 4, the selected parameters which are θ_1 , θ_2 , θ_3 and L are determined due to their significant impact on flow direction and velocity within the runner. The optimization problem can be formulated as:

$$\text{Objective function} = f(\theta_1, \theta_2, \theta_3, L) \tag{1}$$

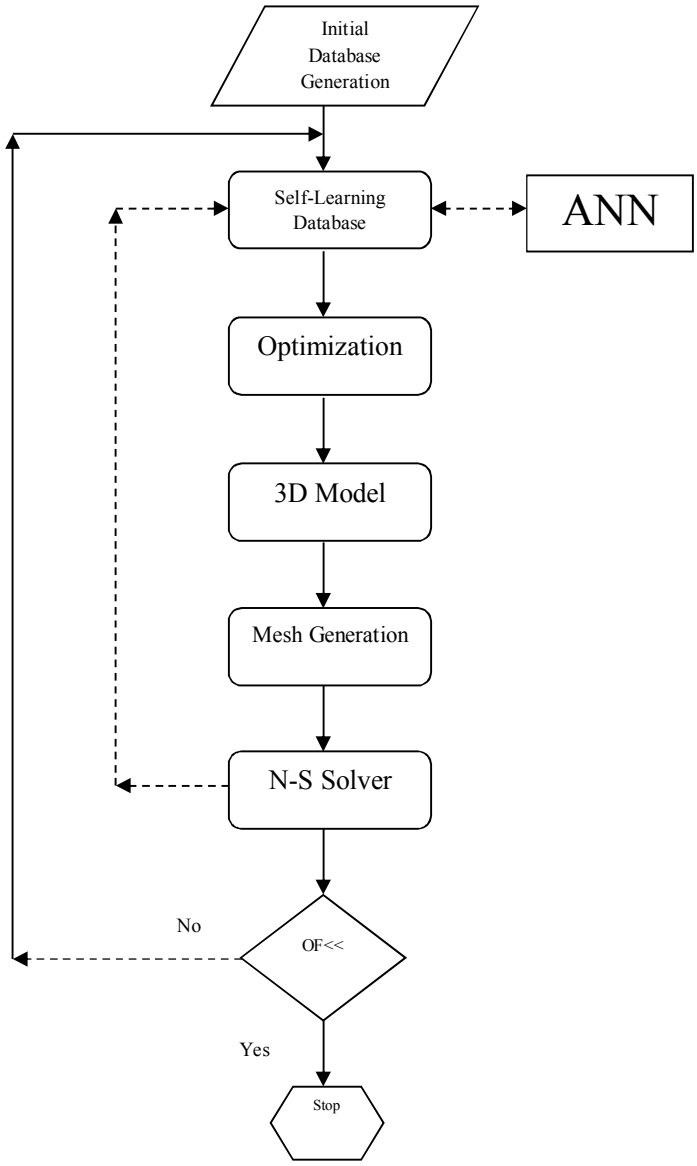

Fig. 3. Numerical optimization technique flowchart

It is noteworthy to accentuate that the runner length is the only parameter of its geometry which is involved in the optimization process. Other variables such as blade angles, number of blades and their profiles are kept intact during the optimization.

Table 1. Optimization parameters and their variation scopes

Parameters	Initial value	Lower bound	Upper bound
θ_1 (deg)	16	13	21
θ_2 (deg)	24	16	30
θ_3 (deg)	11	4	17
L (m)	0.1776	0.15	0.185

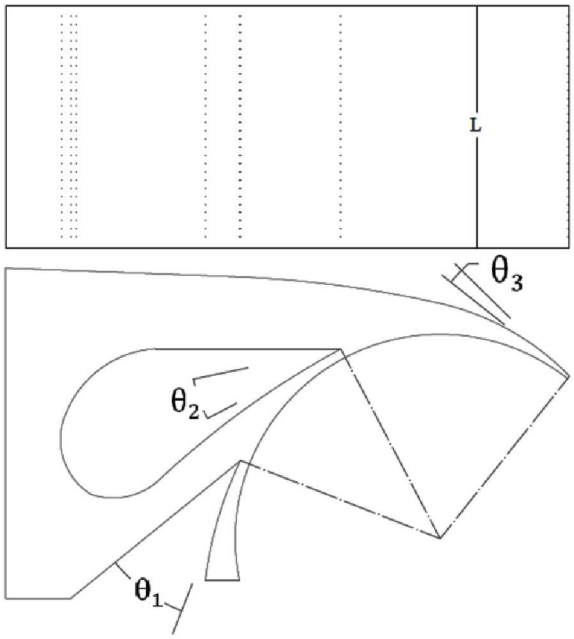

Fig. 4. Selected optimization parameters

4.2. Numerical investigation

Flow simulations were entirely performed by means of a commercial 3D Navier-Stokes CFD code which uses the finite element based finite volume discretization method. Based on the operating condition two phase flow simulations were performed. A coupled method was exploited to solve the governing equations, meaning that the equations of momentum and continuity were solved simultaneously. In order to calculate the free surface, the volume of fluid (VOF) method and homogenous multiphase model was exploited. In homogeneous multiphase flow, a common flow field is shared by all fluids, as well as other relevant fields such as temperature and turbulence. This allows some simplifications to be made to the multi fluid model resulting in the homogeneous model. For a given transport process, the homogeneous model assumes that the transported quantities (with the exception of volume fraction) for that process are the same for all phases, that is,

$$\varphi_\alpha=\varphi \quad 1\leq \alpha \leq N_p, \tag{2}$$

where N_p is total number of phases, and φ is a general scalar variable. Because transported quantities are shared in homogeneous multiphase flow, it is sufficient to solve for the shared fields using bulk transport equations rather than solving individual phasic transport equations. The bulk transport equations can be derived by summing the individual phasic transport equations over all phases to give a single transport equation for φ:

$$\frac{\bar{\partial}}{\partial t}(\rho\varphi) + \nabla.(\rho U\varphi - \Gamma\,\nabla\varphi) = S \tag{3}$$

where

$$\rho = \sum_{\alpha=1}^{N_p} r_\alpha \rho_\alpha \tag{4}$$

$$U = \frac{1}{\rho}\sum_{\alpha=1}^{N_p} r_\alpha \rho_\alpha U_\alpha \quad (5)$$

$$\Gamma = \sum_{\alpha=1}^{N_p} r_\alpha \Gamma_\alpha \quad (6)$$

S denotes a source term, r is volume fraction, ρ is material density, Γ is diffusivity, and U is velocity magnitude. The subscript α denotes that the quantity applies to phase α (Hirt & Nichols, 1981). As a convergence criterion, the computations were continued until the global residuals decreased to less than 10^{-5} for discretized equations.

4.3. Solution Parameters

In order to achieve more accurate and robust results, the RNG k-ε turbulence model, which is based on renormalization analysis of Navier-Stokes equations, was employed (Speziale & Thangam 1992; Castilla et al., 2010). The rapidly straining flow and high streamline curvatures, which are present in this case study, necessitate the use of the RNG k-ε turbulence model (Yakhot et al., 1992). The mechanical loss resulting from seals and bearings are calculated according to (Nechleba, 1980).
Total pressure and mass flow rate were imposed in inlet and outlet respectively and an opening with atmospheric condition was imposed to the air valve as indicated in Fig. 5. No-slip condition with 150μm sand grain roughness was assumed for rotor wall and 260μm was assumed for other walls exposed to fluid flow based on their surface material (Munson et al., 1990).

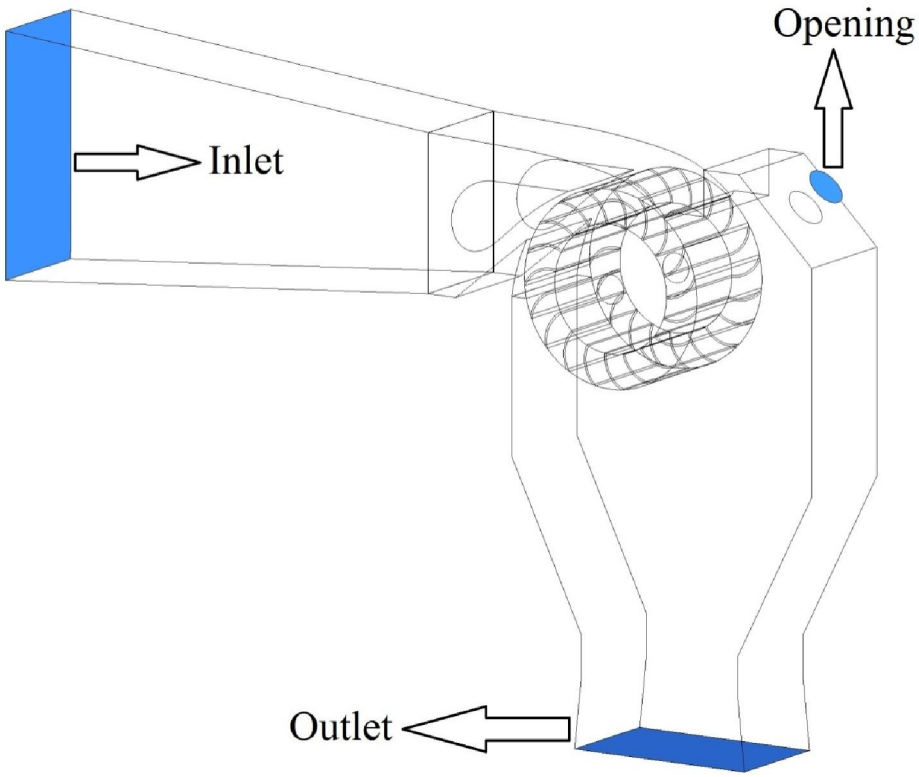

Fig. 5. Schematic of computational domain and boundary conditions

4.3.1. Grid Generation

With the aim of generating a structured hexahedral grid, the solution domain was divided into four component parts: turbine inlet extension, nozzle, runner, casing and draft tube. The independence of

turbine's hydraulic efficiency from grid number was checked, as depicted in Fig. 6. It was found that efficiency varies by less than 0.5%when grid numbers are more than 0.75 million. Table 2 lists the final grid numbers of each component.

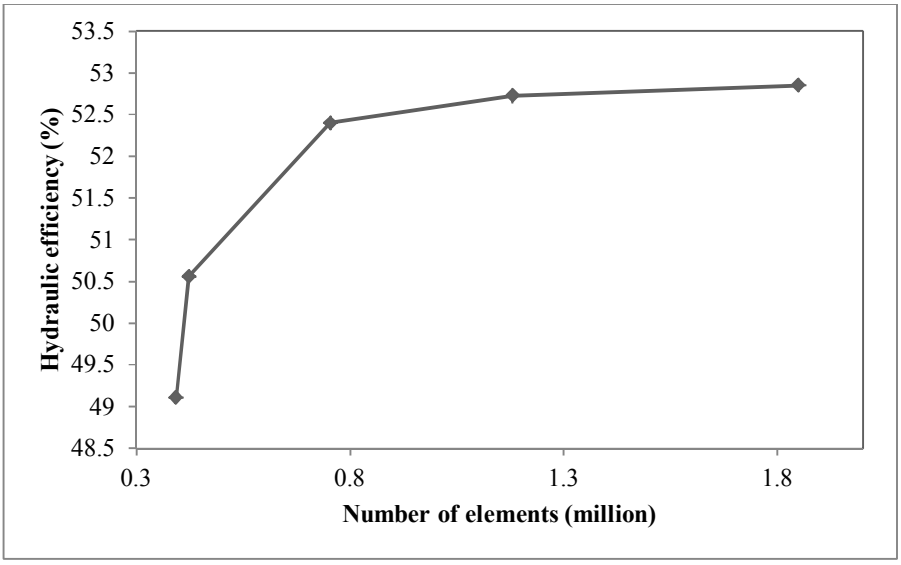

Fig. 6. Hydraulic efficiency versus grid number

Table 2. Grid numbers of each component

Component	Number of elements
Inlet extension	29000
Nozzle	130300
Runner	412405
Casing and draft tube	182257
Total number of elements	753962

4.3.2. Verification of CFD results

Fig. 7 illustrates the efficiency and output power curves of initial geometry extracted from experimental and CFD results. It can be observed that the maximum difference in hydraulic efficiency and output power, within the scope of 0.7-1.3$n_{\text{Best Efficiency Point (BEP)}}$, are 2.33 % and 2.75 kW, respectively. In addition, the errors between predicted hydraulic efficiency and power and experimental values at BEP are 0.79 % and 0.93 kW, respectively. This demonstrates that CFD could be used to predict cross-flow turbine performance with an acceptable accuracy.

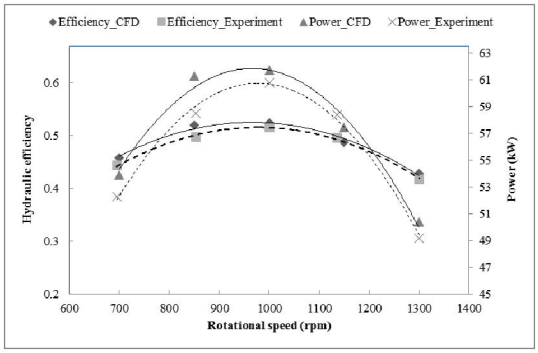

Fig. 7. Performance curves of experimental and CFD results (Pasandideh Pour, 2012)

4.3.3. CFD results analysis

Using available CFD results of initial geometry an investigation on the flow direction and hydraulic loads on the shaft were performed. Fig. 8 and Fig. 9 illustrate water volume fraction and velocity contours respectively on the mid plane cross section of the turbine. As shall be observed the water jet within the runner impacts the turbine shaft resulting in an alternating hydraulic force on the shaft, which may be the cause of its fatigue failure.

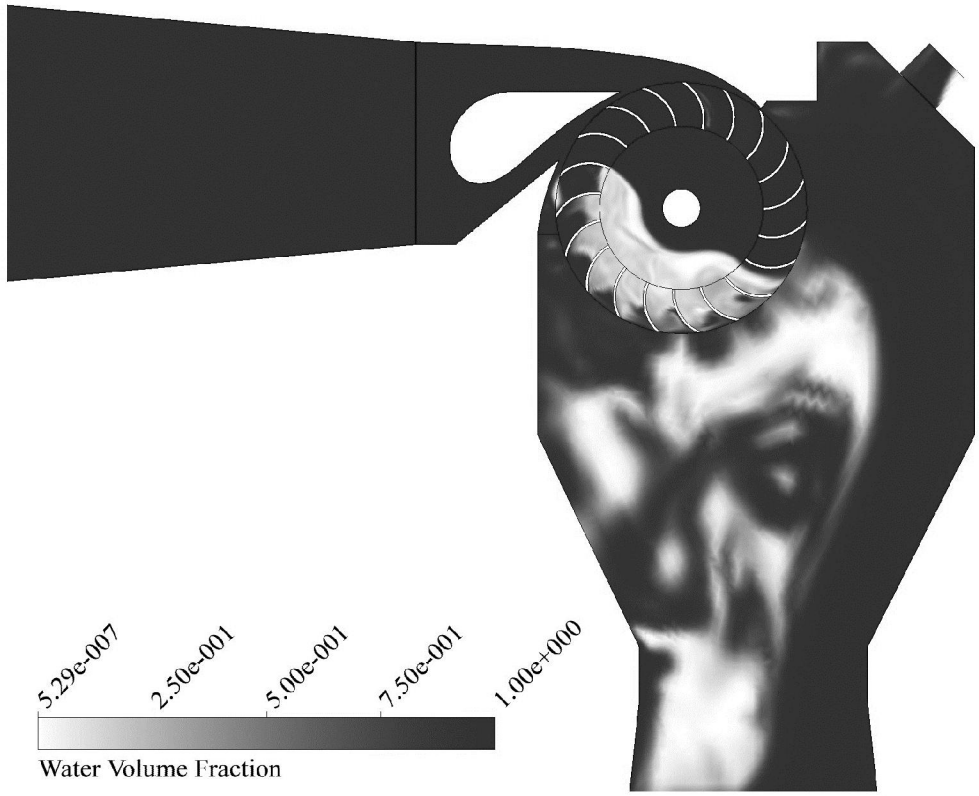

Fig. 8. Water volume fraction contour inside the turbine

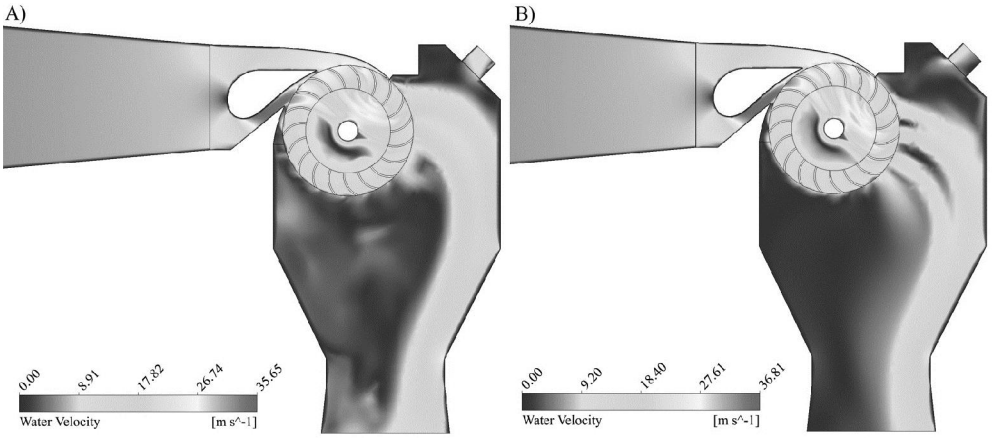

Fig. 9. Velocity contours of A) initial B) optimal geometry (K_e= *0.05)*

Fig. 10 depicts hydraulic loading distribution along the shaft axis. In the following steps of optimization we attempted to alter the flow direction in the runner in order to decline its impact on the shaft in conjunction with improving turbine hydraulic efficiency.

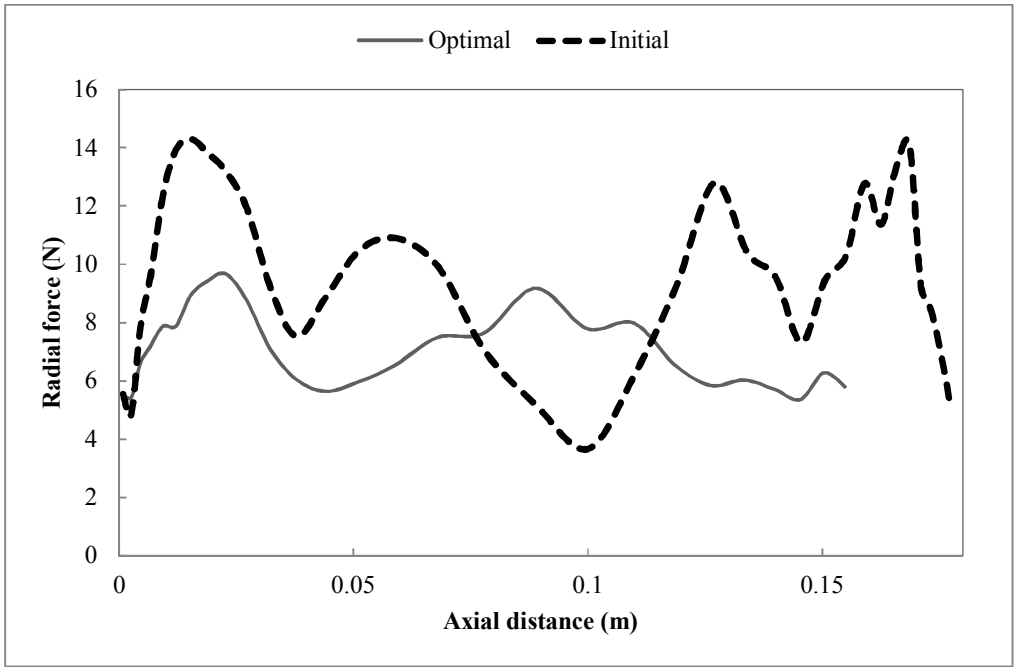

Fig. 10 Axial distribution of hydraulic load on the initial and optimal turbine shaft

4.4. Shaft stress analysis

In order to quantize the fatigue life of the shaft it is necessary to calculate the shaft fatigue factor of safety which is based on stress analysis. Due to the simplicity of shaft geometry an analytical approach would be accurate enough to be exploited. Using DE-ASME Elliptic (Eq. 7) as an analytical approach for shaft fatigue life calculation proposed by Budynas et al. (Budynas et al., 2008) the factor of safety is determined.

$$\frac{1}{n}=\frac{16}{\pi d^3}\left[4\left(\frac{K_f M_a}{S_e}\right)^2+3\left(\frac{K_{fs}T_a}{S_e}\right)^2+4\left(\frac{K_f M_m}{S_y}\right)^2+3\left(\frac{K_{fs}T_m}{S_y}\right)^2\right]^{\frac{1}{2}} \tag{7}$$

where n is the shaft factor of safety (FOS), d is the shaft diameter, K_f and K_{fs} are fatigue stress-concentration factors in bending and torsion respectively, M_a and T_a are alternating bending moment and torsional torque respectively, M_m and T_m are mean bending moment and torsional torque, S_e is the corrected endurance limit and S_y is yield strength. In order to obtain loading parameters such as bending moment and torsional torque a static analysis is required, thus the pressure profile on the shaft surface resulted from CFD is extracted and a simple code was exploited to integrate the pressure values to calculate forces.

4.5. Artificial Neural Networks

The optimization method is based on the use of Artificial Neural Networks (ANNs). ANNs are used for the construction of meta-models of each constraint or objective function within an optimization process. They are chosen mainly for one reason; the use of a meta-model allows the calculations to be performed in parallel, with a consequential reduction of the overall timescale of the activity. A neural network with hidden and output layer architecture was used for function approximation. The hidden layer size is specified to reach an acceptable approximation and may vary for each case. The meta-model was exploited to approximate both the hydraulic efficiency and the factor of safety concerning shaft fatigue life based on four mentioned geometrical parameters. The training process of ANN is

performed using efficiency and shaft factor of safety obtained from CFD results for initial population of 26 samples which were selected using statistical Box-Behnken (Box & Behnken, 1960) method in order to be a more suitable representative of overall population. Due to limited computational resources establishing a fine global database is unattainable, thus in each iteration the database is only developed locally around the output point of the optimization (Derakhshan et al., 2013).

4.6. Genetic algorithm

Genetic algorithm (GA) is the most popular type of evolutionary algorithm (EA). The basic idea underlying the method comes from the behavior of living organisms in nature. An initial set of individuals, called initial population, undergoes a natural selection process. So each individual can be seen as a DNA string. Parental populations give birth to offsprings. GAs work on individuals as coded bit strings, thus they need discrete variable intervals. The new generations are created following a series of genetic rules (Thévenin & Janiga, 2008):

- Selection
- Mutation
- Crossover

In this study, a double-vector GA with population size of 20 was utilized. Deviation of 10^{-6} for objective function was set as a stoppage criterion.

4.7. Objective function

The optimization process is based on increasing hydraulic efficiency and improving shaft fatigue life which are simultaneously optimized with respect to design parameters. The optimization objective function is imposed on the operating point to increase the efficiency and shaft FOS. This objective function is expressed as:

$$OF = \eta + K_e.n \tag{8}$$

where η is hydraulic efficiency and is defined as:

$$\eta = \frac{\tau\omega}{\dot{m}gH} \tag{9}$$

where τ and ω are shaft torque and rotational speed respectively, and $\dot{m}gH$ is the net hydraulic power. K_e is a linear factor that defines the weight of each part of the objective function and is rather an arbitrary factor that is mainly based on the discretion of the designer. In order to evaluate the effect of this parameter, four distinct values of K_e= *{0, 0.05, 0.2, 0.5}* are investigated in the optimization process. This parameter determines the maximum scarification of efficiency to obtain higher FOS. For instance the value of K_e= *0.05* would result in a maximum 4% reduction in hydraulic efficiency.

5. Optimization results

The convergence history of the optimization procedure for K_e= *0.05* has been shown in Fig.11. It can be observed that with the increase of iterations, the error between the artificial neural network predictions and the CFD results diminishes, and that both curves converge after 22 iterations.

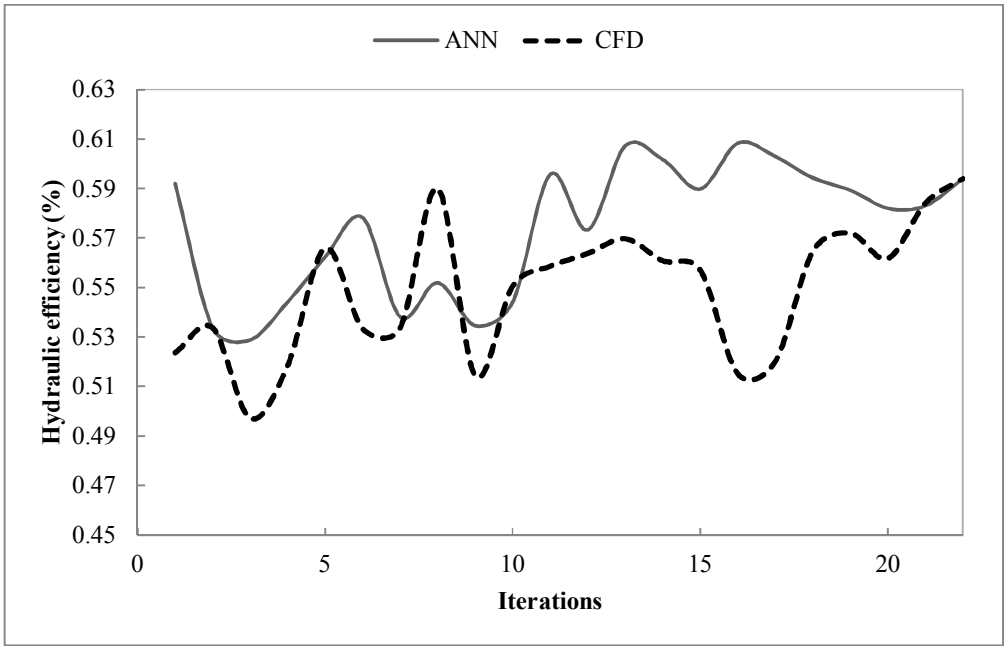

Fig. 11 Convergence history of optimization procedure (K_e= *0.05)*

The corresponding computation time was approximately 350 hours for each case of optimization process when using a PC with Intel Core i5 chip, 2.67 GHz of speed and 4GB of RAM memory. The optimization results of KTP-B60 turbine have been shown in Table 3 for the initial and final geometry. As it is shown in Table 3 the hydraulic efficiency and shaft fatigue factor of safety have improved from 52.26 % to 62.40 % and from 0.967 to 1.014 respectively.

Table 3. Initial and optimal turbine parameters

	θ_1 *(deg)*	θ_2*(deg)*	θ_3*(deg)*	*L(m)*	Efficiency (%)	Power (kW)	FOS
Initial	16	24	11	0.1776	52.26	61.52	0.967
Optimal *(K_e=0.05)*	15.51	23.27	9.61	0.1550	62.40	73.46	1.014

A more than unity factor of safety in DE-ASME Elliptic, which is considered as a relatively moderate method in fatigue analysis, indicates infinite shaft life, albeit there are several other factors involved in this issue. Fig. 12 depicts the visual comparison between initial and optimal geometry. By altering the K_e factor in the objective function the designer would be able to change the priorities of each objective parameter in the optimization procedure.

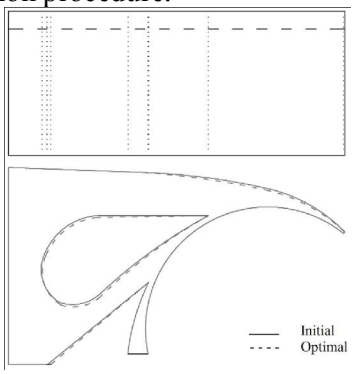

Fig. 12 Visual comparison of initial and optimal geometry

As can be observed in Table 4 increasing the factor K_e would result in a higher FOS and relatively reduced efficiency. For instance in the scope of $K_e = 0 – 0.5$ the FOS was increased by 28.8 % and the hydraulic efficiency was declined by 29.34 %.

Table 4. Optimization results for different values of K_e

K_e	θ_1 (deg)	θ_2(deg)	θ_3(deg)	L(m)	Efficiency (%)	Power (kW)	FOS
0	15.31	23.17	12.25	0.152	63.73	75.02	0.948
0.05	15.51	23.27	12.39	0.1550	62.40	73.46	1.014
0.2	14.964	22.63	12.43	0.160	60.65	71.40	1.052
0.5	20.748	29.32	12.52	0.173	45.03	53.01	1.221

As can be observed in Table 3 and Fig. 12 there are some major differences in the initial and improved geometry such as turbine length, which has been reduced significantly resulting in a lower nozzle throat area that increases velocity retrieval from upstream pressure. As indicated in velocity contours of Fig. 9 this also would increase the wall effect and pressure loss. In addition to the abovementioned modification, nozzle angles have been altered to improve flow path. For instance the upper angle (θ_3) of the nozzle has been increased which resulted in reduction of non-crossover portion of the flow. Non-crossover is the portion of water jet that does not cross the runner (Pasandideh Pour, 2012). However the excessive increase in this parameter would disturb the flow pattern inside the runner, thus it can be concluded from these examples that the optimal geometry is a compromise between diversity of factors affecting the objective function. A comparison of hydraulic load distribution on shaft is available in Fig. 10, which indicates a decline in overall hydraulic loading in optimal turbine. Results indicate an improvement in the turbine efficiency and shaft FOS, thus the proposed method could be exploited as a beneficial approach in optimization of cross-flow hydraulic turbines.

6. Conclusion

An efficient and low cost approach was developed and applied to the optimization of micro cross flow turbines. The proposed procedure consists of the usage of an artificial neural network (ANN) during the optimization phase, which allows for the application of optimization algorithms in an efficient way. The originality of this study lies in the synthesis of mechanical and hydraulic parameters that have major impact on the turbine performance and endurance. The selected objective function allows for efficiency and shaft fatigue FOS improvement simultaneously. The optimized turbine geometry was simulated by means of a validated (using available experimental data for initial geometry) 3D two phase flow solver. Numerical simulation results showed efficiency and relative shaft fatigue FOS improvement of 10.14% and 4.86 % for KTP-B60 turbine which would result in a significant improvement in achievable hydro energy capacity within the range of micro hydraulic turbines.

References

Banki, D. (1918). NeueWasser turbine, *Turbienwesen*, Nos 21-24.

Box, G. E., & Behnken, D. W. (1960). Some new three level designs for the study of quantitative variables. *Technometrics*, 2(4), 455-475.

Budynas, R. G., & Nisbett, J. K. (2008). *Shigley's mechanical engineering design*. New York: McGraw-Hill.

Castilla, R., Gamez-Montero, P. J., Ertürk, N., Vernet, A., Coussirat, M., & Codina, E. (2010). Numerical simulation of turbulent flow in the suction chamber of a gear pump using deforming mesh and mesh replacement. *International Journal of Mechanical Sciences*, 52(10), 1334-1342.

Choi, Y. D., Lim, J. I., Kim, Y. T., & Lee, Y. H. (2008). Performance and internal flow characteristics of a cross-flow hydro turbine by the shapes of nozzle and runner blade. *Journal of Fluid Science and Technology*, 3(3), 398-409.

Costa Pereira, N. H., & Borges, J. E. (1996). Study of the nozzle flow in a cross-flow turbine. *International journal of mechanical sciences*, 38(3), 283-302.

Demeulenaere, A., Ligout, A., & Hirsch, C. (2004). Application of multipoint optimization to the design of turbomachinery blades. *ASME*.

Derakhshan, S., Mohammadi, B., & Nourbakhsh, A. (2008). Incomplete sensitivities for 3D radial turbomachinery blade optimization. *Computers & Fluids*, 37(10), 1354-1363.

Derakhshan, S., & Nourbakhsh, A. (2008). Experimental study of characteristic curves of centrifugal pumps working as turbines in different specific speeds. *Experimental thermal and fluid science*, 32(3), 800-807.

Derakhshan, S., Pourmahdavi, M., Abdolahnejad, E., Reihani, A., & Ojaghi, A. (2013). Numerical Shape Optimization of a Centrifugal Pump Impeller Using Artificial Bee Colony Algorithm. *Computers & Fluids*.

Desai, V. R., & Aziz, N. M. (1994). An experimental investigation of cross-flow turbine efficiency. *Journal of Fluids Engineering*; (United States), 116(3).

Fiuzat, A. A., & Akerkar, B. P. (1991). Power outputs of two stages of cross-flow turbine. *Journal of Energy Engineering*, 117(2), 57-70.

Fiuzat, A. A., & Akerkar, B. (1989, August).The use of interior guide tube in cross flow turbines. In *Waterpower*'89 (pp. 1111-1119). ASCE.

Furukawa, A., Okuma, K. (1995). Extra-low head hydro power utilization with Darrieus type runner, *Turbomachiney*, 30, 142–146.

Hirt, C. W., & Nichols, B. D. (1981).Volume of fluid (VOF) method for the dynamics of free boundaries. *Journal of computational physics*, 39(1), 201-225.

Inagaki, A., & Kanemoto, T. (2005). Development of Gyro-Type Hydraulic Turbine Suitable for Shallow Stream (2nd Report, Flow Conditions and Rotor Works). *Nippon Kikai Gakkai Ronbunshu B Hen (Transactions of the Japan Society of Mechanical Engineers Part B)(Japan)*, 17(4), 1092-1098.

Kanemoto, T., Furukawa, A., Ikeda, T., & Iio, S. (2007). Research and development on hydroelectric units for micro-hydro power utilization. *In Proceedings of the 2007 small hydropower/ocean energy international co-seminar and sixth hydropower technical association seminar* (pp. 3-7).

Kanemoto, T., Inagaki, A., Misumi, H., & Kinoshita, H. (2004). Development of gyro-type hydraulic turbine suitable for shallow stream (1st report, rotor works and hydroelectric power generation). *Nippon Kikai GakkaiRonbunshu B Hen (Transactions of the Japan Society of Mechanical Engineers Part B) (Japan)*, 16(2), 413-418.

Khosrowpanah, S., Fiuzat, A. A., & Albertson, M. L. (1988). Experimental study of cross-flow turbine. *Journal of Hydraulic Engineering*, 114(3), 299-314.

Kosnik, L. (2008). The potential of water power in the fight against global warming in the US. *Energy Policy*, 36(9), 3252-3265.

Lal, J. (1961). *Hydraulic machines*. Metropolitan Book Company.

Matsuura, K., Okuma, K., Watanabe, S., & Furukawa, A. (2006). Operation characteristics of ducted Darrieus turbine for extra-low head hydropower. *Proceedings of renewable energy*, CD-ROM ON-4-5, 2732-4.

Munson, B. R., Young, D. F., & Okiishi, T. H. (1990). *Fundamentals of fluid mechanics*. New York.

Nakajima, M., Iio, S., & Ikeda, T. (2008). Performance of double-step Savonius rotor for environmentally friendly hydraulic turbine, *Journal of Fluid Science and Technology*, 3, 410–419.

Nakajima, M., Iio, S., & Ikeda, T. (2008). Performance of Savonius rotor for environmentally friendly hydraulic turbine. *Journal of Fluid Science and Technology*, 3(3), 420-429.

Nechleba, M. (1980). *Hydraulic turbine-design and equipment*, ARTIA Prague.

Nourbakhsh, A., Safikhani, H., & Derakhshan, S. (2011). The comparison of multi-objective particle swarm optimization and NSGA II algorithm: applications in centrifugal pumps. *Engineering Optimization*, 43(10), 1095-1113.

Pasandideh Pour, M. (2012).Numerical simulation of Cross-Flow turbine, M.Sc. thesis, Iran University of Science and Technology.

Penche, C. (1994). *Layman's Guidebook on how to Develop a Small Hydropower Site*, Commission of the European Communities.

Phommachamh, D., Kurokawa, J., Choi, Y. D., Nakajima, N., & Motohashi, T. (2006). Development and performances of a micro positive displacement hydropower turbine. *Turbomachinery*, 34(10), 621-11.

Shepherd, D. G. (1956). *Principles of turbomachinery*. Macmillan.

Speziale, C. G., & Thangam, S. (1992). Analysis of an RNG based turbulence model for separated flows. *International Journal of Engineering Science*, 30(10), 1379-IN4.

Takamatsu, Y., Furukawa, A., Okuma, K., & Takenouchi, K. (1991). Experimental studies on a preferable blade profile for high efficiency and the blade characteristics of Darrieus-type cross-flow water turbines. *JSME international journal. Ser. 2, Fluids engineering, heat transfer, power, combustion, thermophysical properties*, 34(2), 149-156.

Thévenin, D., & Janiga, G. (Eds.).(2008). *Optimization and computational fluid dynamics*. Springer.

Yakhot, V., Orszag, S. A., Thangam, S., Gatski, T. B., & Speziale, C. G. (1992). Development of turbulence models for shear flows by a double expansion technique. *Physics of Fluids A: Fluid Dynamics*, 4, 1510.

Yassi, Y. (2010). Improvement of the efficiency of the Agnew micro hydro turbine at part loads due to installing guide vanes mechanism. *Energy Conversion and Management*, 51(10), 1970-1975.

Yassi, Y. (2009). The effects of improvement of the main shaft on the operating conditions of the Agnew turbine. *Energy Conversion and Management*, 50(10), 2486-2494.